The role of water in pyrolysate composition and silylation efficiency during analytical reactive pyrolysis of glucans

Marco Mattonai*, Erika Ribechini

Department of Chemistry and Industrial Chemistry, University of Pisa, Via G. Moruzzi 13, 56124 Pisa, Italy

*corresponding author. Mail: m.mattonai@gmail.com

Abstract

The pyrolytic behaviour of two oligosaccharides – cellobiose and cellohexose – was studied using reactive pyrolysis-GC/MS with *in situ* hexamethyldisilazane derivatisation. Pyrolysis was conducted in a sealed vessel at various times ranging from 0.2 to 60 min. Semi-quantitative calculations were carried out on integrated peak areas to obtain information on derivatisation efficiency and composition of the pyrolysate as a function of pyrolysis time. The results were compared with a previous work by us in which glucose and cellulose were studied with the same procedure. Semi-quantitative calculations were carried out to obtain information on the composition of the pyrolysate as a function of pyrolysis time. The derivatisation efficiency was also evaluated by measuring the yield of fully-derivatised anhydrosugars as a function of pyrolysis time. The derivatisation efficiency was found to increase with the increase of the degree of polymerisation of the substrate. The influence of a sealed environment and free water molecules released during the pyrolysis process were highlighted and compared with the literature, in order to account for the observed differences in pyrolytic yields and derivatisation rates.

Keywords: Carbohydrates; Analytical pyrolysis; In situ derivatisation; Gas chromatography

1. INTRODUCTION

Pyrolysis of lignocellulosic biomass is currently under the spotlight due to its promising potential for a sustainable production of fuels and chemicals [1,2]. Many factors influence the pyrolysis mechanism of lignocellulose, and especially of its cellulosic fraction, including sample preparation, crystallinity, degree of polymerization, and the presence of inorganics [3-5]. Analytical pyrolysis coupled to gas-chromatography-mass spectrometry (Py-GC/MS) has risen among the staple techniques for the study of cellulose pyrolysis [1,6-8] due to its ability to provide information on the sample without requiring any pre-treatment. The main challenge posed by this technique is that cellulose pyrolysis products bear polar functional groups, which are not efficiently retained by common GC stationary phases.

Derivatisation has proven to be an effective strategy to improve the chromatographic quality by converting groups bearing mobile hydrogen into less polar ones [9]. One of the most traditional derivatisation strategies is silylation [9-11], but its main disadvantage is the low reaction rate, which usually results in partial derivatisation of the compounds bearing more than one mobile hydrogen group [12,13]. Partial derivatisation increases the number of peaks in the chromatogram without adding information, and therefore it should be avoided.

A possible solution to partial derivatisation is to extend the contact time between the pyrolysis products and the derivatising agent. In a previous paper, we used a micro reaction sampler to extend the reaction time during analytical pyrolysis of glucose and cellulose with in situ hexamethyldisilazane derivatisation [14,15]. Thanks to this instrumental setup, partial derivatisation was overcome after 30 min of pyrolysis.

Glucose and cellulose showed different reactivity towards hexamethyldisilazane, and the necessity of further studies in this direction was addressed [14]. These studies should especially focus on establishing how all parameters can affect the derivatisation process inside the micro reaction sampler. This includes external factors such as the closed environment and high pressure, and

internal factors such as the presence of pyrolysis products like water [16,17], which are forced to stay in close contact with the pyrolysis mixture and the derivatising agent.

In the present work, the results obtained in the previous paper are expanded with new data regarding the analysis of two additional glucans, cellobiose and cellohexose, in order to improve our knowledge on the factors affecting the derivatisation process. The two new substrates were pyrolyzed at different times, and compositional and kinetic data were obtained from semi-quantitative calculations. New data regarding glucose and cellulose were also obtained from kinetic analysis of the derivatisation process. The results were explained by hypothesising a role of water in the system, and the hypothesis was discussed in comparison with the available literatures. This work is to be considered as a follow-up on the results presented in the previous paper dealing with glucose and cellulose.

2. MATERIALS AND METHODS

2.1 Samples and materials: D-(+)-glucose (99.5%, Sigma-Aldrich, USA), D-(+)-cellobiose (≥ 98%, Sigma-Aldrich, USA), D-(+)-cellohexose (Santa Cruz Biotechnology, USA) and Sigmacell cellulose (type 101, Sigma-Aldrich, USA) were used as substrates. The substrates were all analysed without further processing. Hexamethyldisilazane (HMDS, 99.9%, Sigma-Aldrich, USA) was used as derivatising agent in all experiments.

2.2 Experimental parameters: Experiments were performed with an EGA/PY-3030D micro-furnace pyrolyser equipped with a PY-1050 Micro Reaction Sampler (Frontier Laboratories Ltd., Japan). A description of this sampler has been provided in previous publications [15,18], and detailed information are provided in the Supplementary Materials. The pyrolyser was connected to a 6890 gas chromatograph equipped with a split/splitless injector and a 5973 mass spectrometric detector (Agilent Technologies, USA). All experiments were performed with a furnace temperature of 400 °C and an interface temperature of 280 °C. The GC injector was operated in split mode with a 20:1 ratio at 280 °C. Separation of the pyrolysis products was achieved using an HP-5MS column (30 m x 0.25

mm, film thickness 0.25 µm, Agilent Technologies, USA) coupled with a deactivated silica pre-column (2 m x 0.32 mm, Agilent Technologies, USA) and using helium as carrier gas (1 mL/min). The following temperature program was used for the GC oven: 50 °C for 1 min, 10 °C/min up to 100 °C, then for 2 min, 4 °C/min up to 190 °C, then for 1 min, 30 °C/min up to 280 °C, then for 30 min. The transfer line to the mass spectrometer was kept at 280 °C. The mass spectrometer was operated in EI positive mode (70 eV, *m/z* range 50-600). The ion source and quadrupole temperatures were 230 °C and 150 °C, respectively. Pyrolysis times were 0.2, 0.5, 1, 2, 5, 10, 20, 30 and 60 min for each sample. In each experiment, 80 µg of sample were directly weighted inside the glass capsule along with 3 µL of HMDS. Before flame-sealing, the glass capsule was put under a gentle stream of nitrogen to ensure inert atmosphere.

2.3 Data processing: Pyrograms were analysed using the Automated Mass spectra Deconvolution and Identification System (AMDIS, version 2.71, NIST, USA). Pyrolysis products were identified based on comparison with previous literature results [10,12,14] and by match with reference mass spectra libraries (Wiley275 and NIST/EPA/NIH, 2002 version). Reproducibility was evaluated by performing experiments at the same pyrolysis times in triplicate. The relative standard deviation was calculated on normalized integrated areas, and was found to be lower than 10%. The kinetic curve fitting calculations were performed using OriginPro 8 (version 8.0724, OriginLab Corporation, USA).

3. RESULTS AND DISCUSSION

3.1 Pyrolysate composition: The pyrograms obtained from cellobiose and cellohexose at all pyrolysis times were processed with the same method that was used for glucose and cellulose in our previous publication [14]. All peaks belonging to identified compounds were integrated, and their areas expressed as percentage of the total pyrogram area. All identified compounds were then grouped into six categories according to their structure and reactions leading to their formation: small molecules, furans, pyrans, cyclopentenones, hydroxybenzenes and anhydrosugars. Full details regarding compound identification and semi-quantitative calculations can be found in the

Supplementary Materials. The percentage areas of peaks belonging to compounds in the same category were added together, giving six total product category yields for each pyrogram. These yields were plotted against the reaction time, and the results are shown in Figure 1.

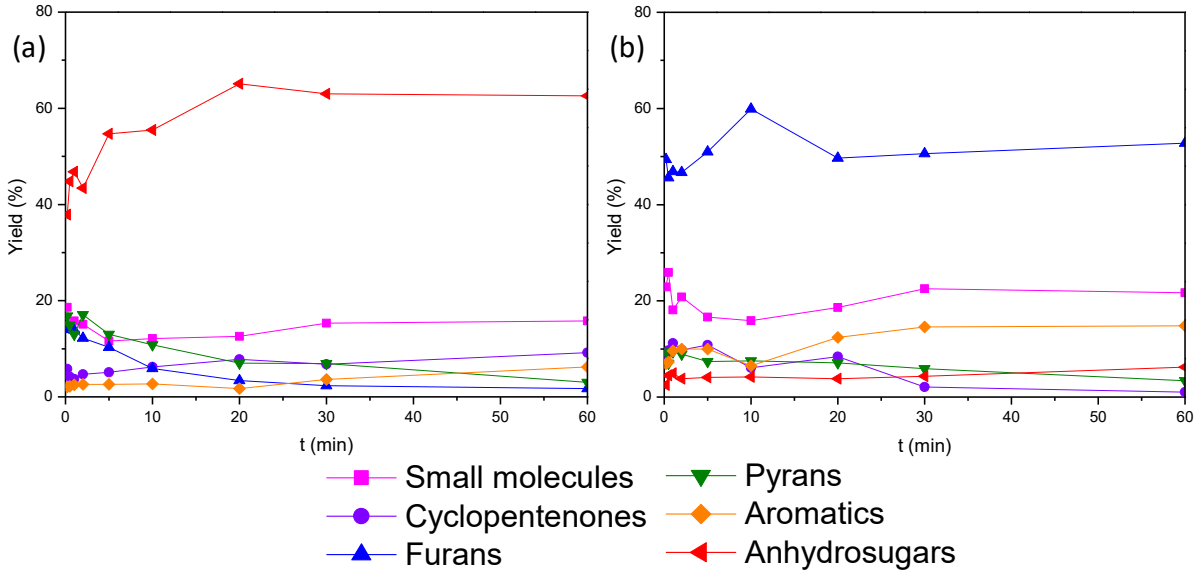

Figure 1: Percentage category yields of the six product categories as a function of pyrolysis time for (a) cellobiose and (b) cellohexose.

The main pyrolysis products of cellobiose were anhydrosugars at all pyrolysis times. This result was close to the one of glucose, although the yield of anhydrosugars for cellobiose was lower. Significant changes in the composition of the pyrolysate took place within the first 20 min of pyrolysis, while the yields tended to remain constant at longer times.

Furans were the most abundant pyrolysis products for cellohexose at all times, while the anhydrosugars yields were always lower than 10%. Small molecules provided the second highet yields, remaining at around 20% throughout the investigated time range. This result brings the behaviour of cellohexose close to the one of cellulose, in which small molecules were the main pyrolysis products at long reaction times.

The comparison of these results with those of glucose and cellulose reflects the increase in the complexity of the pyrolysis mechanism as the degree of polymerisation of the substrate increases.

Moreover, the results suggest a decreasing trend of the anhydrosugars yields with the increase of the molecular weight of the sample. As briefly discussed in our previous publication, this result is surprising, as glucans with high degrees of polymerisation are known to give higher yields of anhydrosugars in conventional fast pyrolysis experiments [19]. The most likely explanation for this difference is that the sealed environment used in our experimental setup can influence the pyrolysis mechanism, by forcing the pyrolysis products to stay in close contact with each other and with the substrate as the pyrolysis process unfolds. A decrease in the yield of levoglucosan was already observed in previous publications when the pressure of the system is increased [20,21].

The high yields of anhydrosugars obtained from glucose and cellobiose suggest that direct water elimination from these substrates is the most favoured raction. This is consistent with the low content of glycosidic bonds in these carbohydrates compared to cellhexose and cellulose. On the other hand, the yield of anhydrosugars for cellohexose and cellulose is very low. According to Mamleev and co-workers [22] and Lu and co-workers [23], the first stage of carbohydrates fast pyrolysis is dominated by transglycosylation, which reduces the degree of polymerisation of the substrate and generates a liquid intermediate composed of oligosaccharides and other small compounds. The formation of a liquid phase was discussed by Ledé in two well-known papers [24,25]. Transglycosylation should lead to the formation of levoglucosan, but further degradation of this product can take place if its residence time in the liquid medium is long enough. This further degradation occurs via a series of secondary reactions, which are catalysed by small pyrolysis products bearing acid hydrogen atoms inside the liquid phase, such as water and small carboxylic acids [22]. It is important to also notice that most of these secondary reactions involve the release of water molecules [26-28]. Varhegy and co-workers showed that water molecules released during pyrolysis of cellulose in a sealed environment can act as catalyst for further degradation of the substrate [29].

In light of these observations, we can attribute the difference in pyrolytic yield between glucose/cellobiose and cellohexose/cellulose to two factors. The first factor is the presence of a

liquid medium in the pyrolysis of cellohexose and cellulose, which is not present in glucose and cellobiose. This liquid medium favours catalytic reactions leading to the formation of small molecules and decreasing the yield of levoglucosan. The second factor is the amount of free water molecules. As water is released in a close environment such as the one we are using, its partial pressure increases, and the release of additional water molecules is hindered. The low yield of secondary pyrolysis products in glucose and cellobiose could therefore also be due to the high amount of water released during the first stage of pyrolysis. On the other hand, secondary reactions are more favoured for cellohexose and cellulose, as the first reaction for these substrates is transglycosylation, which does not involve water release.

Additional insights into the role of water in these experiments can be obtained by taking a closer look at the derivatisation process, which will be discussed in the next section.

3.2 Anhydrosugars derivatisation: The derivatisation process was studied in detail by looking at the anhydrosugars category, to obtain more information on the efficiency of HMDS as a silylating agent in all four cases. This compound category is particularly subject to partial derivatisation, as all anhydrosugars present three hydroxy groups, and therefore the yields of the single anhydrosugars are significantly affected by the derivatisation efficiency. Nine different compounds belong to the anhydrosugars category, and their structures are presented in Figure 2. All anhydrosugars present three spatially close hydroxy groups, making this compound category particularly subject to partial derivatisation. In fact, these compounds can be further classified on the basis of the number of hydroxy groups that have been derivatised. Following the same data processing method of the previous paper, the percentages of mono-, bi- and tri-derivatised anhydrosugars were calculated as a function of pyrolysis time for cellobiose and cellohexose. The results are presented in Figure 3. The results obtained from cellobiose were similar to those obtained for glucose. The amount of mono-derivatised anhydrosugars was always lower than 20%, but their presence could still be detected after 2 min of pyrolysis. On the contrary, mono-derivatised anhydrosugars could not be

found even at the shortest pyrolysis time in the pyrograms of cellohexose. This result is similar to the one observed for cellulose, in which mono-derivatised anhydrosugars were found only at 0.2 and 0.5 min of pyrolysis.

The combination of these results and those obtained in the previous work suggest that even the derivatisation process follows a complex path in this reaction system. The data obtained from all four substrates sugest that the derivatisation process can be roughly divided into two stages. In the first stage, derivatisation occurs while the substrate has not yet undergone its thermal degradation. In this stage, derivatisation affects the substrate while it is still mostly intact, and therefore its efficiency can be influenced by steric hindrance of the polysaccharide chain, as well as by the hydrogen bond network between hydroxy groups of the substrate. This means that the derivatisation of the heaviest substrates such as cellulose is less extensive than the one for glucose and cellobiose. This is reflected in the results obtained at the shortest pyrolysis times (0.2 and 0.5 min). The second stage takes place in parallel with the pyrolysis of the substrate, and therefore derivatisation directly affects the pyrolysis products. The results obtained at long pyrolysis times suggest that in this stage there is an inversion in the trend of the derivatisation efficiency, as the anhydrosugars coming from the lighter substrates require more time to achieve complete persilylation than those coming from the heavier substrates.

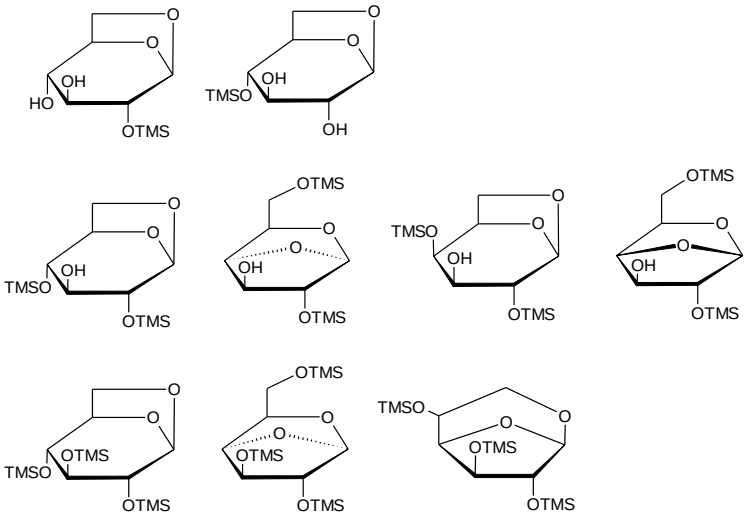

191

192 ***Figure 2:*** Structures of mono-derivatised (first row), bi-derivatised (second row) and tri-derivatised
193 (third row) anhydrosugars identified in the pyrograms of all glucans.

194

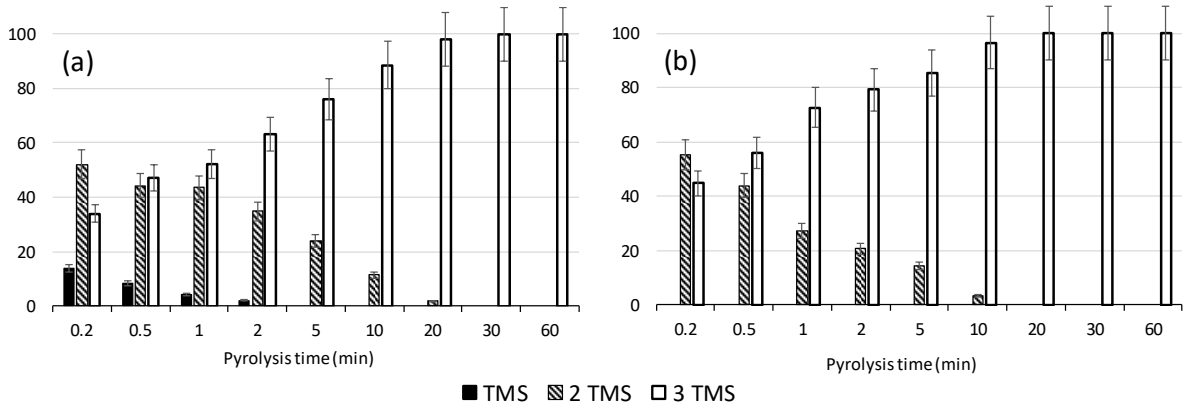

195

196 ***Figure 3:*** Percentage yields of mono-, bi- and tri-derivatised anhydrosugars as a function of pyrolysis
197 time for (a) cellobiose and (b) cellohexose.

198

199 To confirm this hypothesis, the kinetics of anhydrosugars derivatisation was evaluated by fitting of
200 the experimental results with a first-order model. The percentage yields of tri-derivatised
201 anhydrosugars Y were fitted as a function of pyrolysis time t using equation (1). In this equation, the
202 term C reflects the amount of tri-derivatised anhydrosugars obtained in the first stage of
203 derivatisation, which is considered to be fast in the observed pyrolysis time frame. The exponential
204 factor k represents the derivatisation efficiency during the second stage. The results of the fitting are
205 shown in Figure 4 and in Table 1, and additional details are provided in the Supplementary Materials.

206

207 (1) $Y = 100 - Cexp(-t/k)$

208

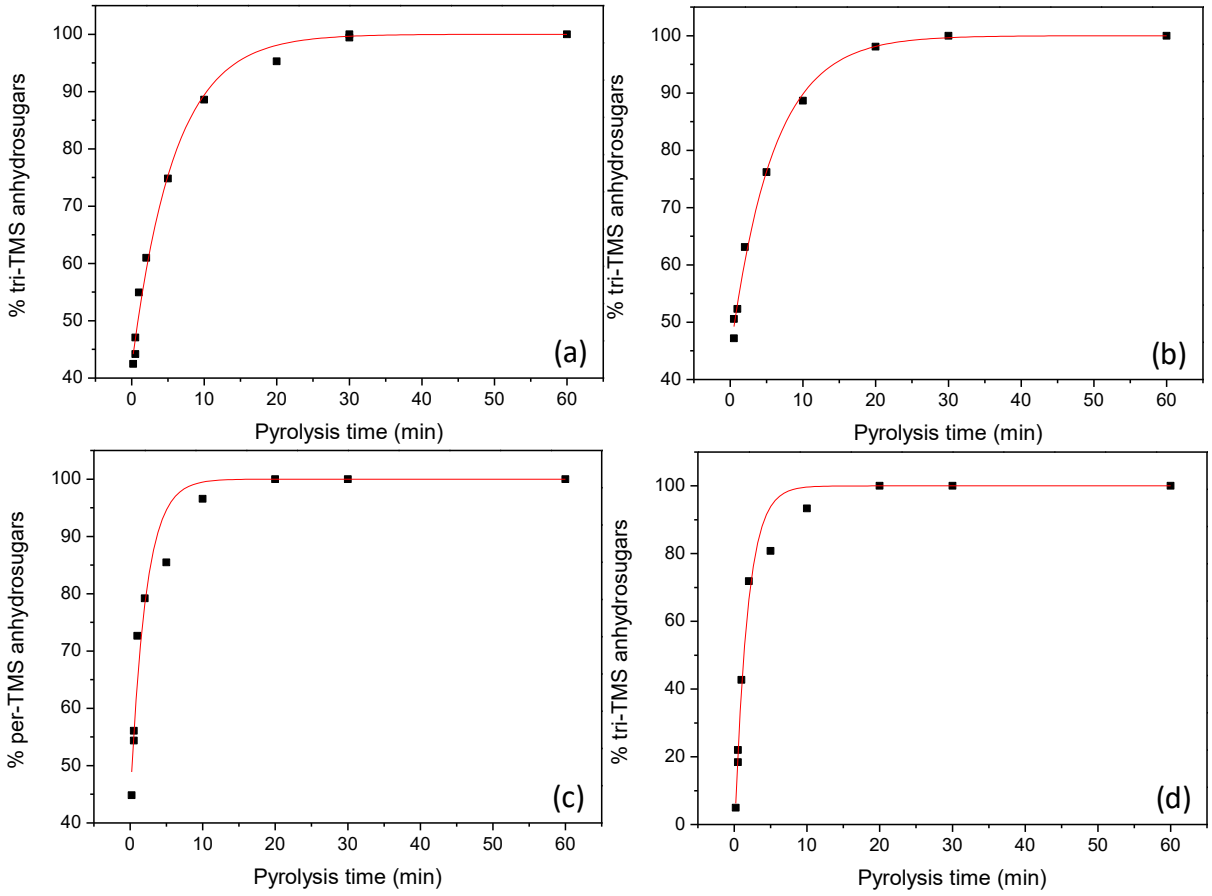

209

210 ***Figure 4:*** Experimental data (dots) and curve fit (lines) of the yields of tri-derivatised anhydrosugars
211 for (a) glucose, (b) cellobiose, (c) cellohexose and (d) cellulose.

212

213 ***Table 1:*** Curve fit parameters and r^2 values for the four substrates.

Sample	C	k	r^2
Glucose	57 ± 1	5.8 ± 0.4	0.99
Cellobiose	59 ± 2	5.1 ± 0.7	0.98
Cellohexose	56 ± 4	2.1 ± 0.4	0.96
Cellulose	105 ± 6	1.8 ± 0.2	0.98

214

215 r^2 values were greater than 0.96 for all fittings. The values of C were close to 60 for glucose,

216 cellobiose and cellohexose, in agreement with the experimental evidence showing that the yield of

217 tri-derivatised anhydrosugars is approximately 40% at the shortest pyrolysis time. On the other

hand, C was approximately 100 for cellulose, indicating that the yield of tri-derivatised anhydrosugars at short pyrolysis times is negligible. This also agrees with the experimental results and with the hypothesis of the first reaction stage. The values of k, on the other hand, decreased significantly going from glucose to cellulose. This decrease was found to be statistically significant using Student's t-test at a 95% confidence, proving that the derivatisation process is less efficient for glucose than for cellulose during the second stage.

While steric hindrance could be used to explain the different derivatisation efficiencies at short pyrolysis times, the trends at long pyrolysis time must be determined by other factors. As for the product yields, we attributed these differences to the presence of water. In fact, free water molecules can readily react with hexamethyldisilazane, generating trimethylsilanol which is no longer reactive towards the mobile hydrogen groups of the substrate [9,30]. The presence of water therefore hinders the derivatisation process.

As observed in the previous paragraph, glucose and cellobiose release a high amount of water by direct elimination during the first stage of pyrolysis. On the contrary, transglycosylation is avoured for cellohexose and cellulose, and the release of water for these substrates is distributed over the course of the whole secondary pyrolysis process. Given these observation, we can hypothesise that the high amount of water released by glucose and cellobiose can hydrolyse HMDS and significantly reduce its apparent derivatisation efficiency. This does not happen with cellulose, in which water is released more gradually and only during the second stage of pyrolysis. Cellohexose showed an intermediate behaviour, as its derivatisation rate was similar to glucose and cellobiose in the first stage (C value), ans close to the one of cellulose in the second stage (k value).

Finally, it is interesting to notice that a complete persilylation of anhydrosugars was obtained in all cases after approximately 20 min of pyrolysis. After this time, the yields of most product categories also remained constant for all substrates. These two results are most likely tied to each other. As discussed in the previous section, changes in the pyrolysate composition are mainly due to secondary reactions involving the loss of water molecules [23,26-28]. However, once the hydroxy

244 groups of the substrates and their pyrolysis products are derivatised, dehydration reactions are
245 hindered and the pyrolysis products cannot be degraded further. This result was also observed in
246 our previous publication [14], in which pyrolysis-silylation of a reference levoglucosan sample in the
247 same experimental conditions yielded only peaks belonging to the whole molecule.
248
249 **4. CONCLUSIONS**
250 The use of reactive pyrolysis with *in situ* silylation allowed us to improve our knowledge on both the
251 derivatisation efficiency and the pyrolysis mechanisms of glucans in a sealed environment. While the
252 substrate and derivatising agent are trapped in the glass vessel, they can react with free water
253 molecules released uring the pyrolysis process. This causes a decrease in the derivatisation rate,
254 which was best observed in the substrates with lowest degrees of polymerisation due to the higher
255 amount of water released in the first pyrolysis step. On the other hand, the formation of a liquid
256 phase during the pyrolysis of the substrates with high degree of polymerisation favoured secondary
257 pyrolysis reactions leading to an increase in the yield of small molecules.
258 The results obtained in this work and the previous paper could be used in the future to drive the
259 pyrolysis process towards the selective production of specific compounds, and to a more efficient
260 use of silylating agents in analytical pyrolysis.
261 Future studies should also establish how the behaviour of glucans under reactive pyrolysis is
262 influenced by the presence of lignin, extractives and other components of lignocellulose.
263
264 **ACKNOWLEDGEMENTS**
265 The University of Pisa is acknowledged for the support under the project “Advanced analytical
266 pyrolysis to study polymers in renewable energy, environment, cultural heritage” (PRA_2018_26).
267 The authors would also like to thank the project “Heterogeneous Robust Catalysts to Upgrade Low
268 value biomass Streams (HERCULES)” funded by the Italian Ministry of Education, Universities and
269 Research (MIUR) within PRIN 2015 call.

REFERENCES

[1] S. Wang, G. Dai, H. Yang and Z. Luo, Lignocellulosic biomass pyrolysis mechanism: A state-of-the-art review; *Progress in Energy and Combustion Science*, 62, (2017) 33-86, https://doi.org/10.1016/j.pecs.2017.05.004.

[2] G. Kabir and B. Hameed, Recent progress on catalytic pyrolysis of lignocellulosic biomass to high-grade bio-oil and bio-chemicals; *Renewable and Sustainable Energy Reviews*, 70, (2017) 945-967, https://doi.org/10.1016/j.rser.2016.12.001.

[3] M. Mattonai, D. Pawcenis, S. del Seppia, J. Łojewska and E. Ribechini, Effect of ball-milling on crystallinity index, degree of polymerization and thermal stability of cellulose; *Bioresource Technology*, 270, (2018) 270-277, https://doi.org/10.1016/j.biortech.2018.09.029.

[4] C. Mukarakate, A. Mittal, P.N. Ciesielski, S. Budhi, L. Thompson, K. Iisa, M.R. Nimlos and B.S. Donohoe, Influence of crystal allomorph and crystallinity on the products and behavior of cellulose during fast pyrolysis; *ACS Sustainable Chemistry & Engineering*, 4, (2016) 4662-4674, https://doi.org/10.1021/acssuschemeng.6b00812.

[5] K. Wang, J. Zhang, B.H. Shanks and R.C. Brown, The deleterious effect of inorganic salts on hydrocarbon yields from catalytic pyrolysis of lignocellulosic biomass and its mitigation; *Applied Energy*, 148, (2015) 115-120, https://doi.org/10.1016/j.apenergy.2015.03.034.

[6] G. SriBala, H.-H. Carstensen, K.M. Van Geem and G.B. Marin, Measuring biomass fast pyrolysis kinetics: State of the art; *Wiley Interdisciplinary Reviews: Energy and Environment*, 8, (2019) e326, https://doi.org/10.1002/wene.326.

[7] G.C. Galletti and P. Bocchini, Pyrolysis/gas chromatography/mass spectrometry of lignocellulose; *Rapid Communications in Mass Spectrometry*, 9, (1995) 815-826, https://doi.org/10.1002/rcm.1290090920.

[8] M.K. Akalın and S. Karagöz, Analytical pyrolysis of biomass using gas chromatography coupled to mass spectrometry; *TrAC Trends in Analytical Chemistry*, 61, (2014) 11-16, https://doi.org/10.1016/j.trac.2014.06.006.

[9] K. Blau and J.M. Halket (Eds.), Handbook of derivatives for chromatography, John Wiley & Sons Ltd, Chichester, 1993, 51-99.

[10] D. Tamburini, J.J. Łucejko, M. Zborowska, F. Modugno, W. Prądzyński and M.P. Colombini, Archaeological wood degradation at the site of Biskupin (Poland): wet chemical analysis and evaluation of specific Py-GC/MS profiles; *Journal of Analytical and Applied Pyrolysis*, 115, (2015) 7-15, https://doi.org/10.1016/j.jaap.2015.06.005.

[11] S.C. Moldoveanu, *Analytical Pyrolysis of Natural Organic Polymers*, Elsevier Science, Amsterdam, 1998, 217-308.

[12] D. Fabbri and G. Chiavari, Analytical pyrolysis of carbohydrates in the presence of hexamethyldisilazane; *Analytica Chimica Acta*, 449, (2001) 271-280, https://doi.org/10.1016/S0003-2670(01)01359-9.

[13] D. Fabbri, G. Chiavari, S. Prati, I. Vassura and M. Vangelista, Gas chromatography/mass spectrometric characterisation of pyrolysis/silylation products of glucose and cellulose; *Rapid Communications in Mass Spectrometry*, 16, (2002) 2349-2355, https://doi.org/10.1002/rcm.856.

[14] M. Mattonai, D. Tamburini, M.P. Colombini and E. Ribechini, Timing in Analytical Pyrolysis: Py(HMDS)-GC/MS of Glucose and Cellulose Using Online Micro Reaction Sampler; *Analytical Chemistry*, 88, (2016) 9318-9325, https://doi.org/10.1021/acs.analchem.6b02910.

[15] A. Hosaka, C. Watanabe, N. Teramae and H. Ohtani, Development of a new micro reaction sampler for pyrolysis-GC/MS system facilitating on-line analytical chemolysis of intractable condensation polymers; *Journal of Analytical and Applied Pyrolysis*, 106, (2014) 160-163, https://doi.org/10.1016/j.jaap.2014.01.014.

[16] J. Scheirs, G. Camino and W. Tumiatti, Overview of water evolution during the thermal degradation of cellulose; *European Polymer Journal*, 37, (2001) 933-942, https://doi.org/10.1016/S0014-3057(00)00211-1.
[17] S.C. Moldoveanu, in S.C. Moldoveanu (Ed.), *Pyrolysis of Organic Molecules with applications to health and environmental issues* Elsevier Science, Amsterdam, 2010, Chapter 16, p. 419-470.
[18] M. Mattonai and E. Ribechini, Fast screening for hydrolysable and condensed tannins in lignocellulosic biomass using reactive Py-GC/MS with in situ silylation; *Journal of Analytical and Applied Pyrolysis*, 135, (2018) 242-250, https://doi.org/10.1016/j.jaap.2018.08.029.
[19] M.S. Mettler, A.D. Paulsen, D.G. Vlachos and P.J. Dauenhauer, The chain length effect in pyrolysis: bridging the gap between glucose and cellulose; *Green Chemistry*, 14, (2012) 1284-1288, 10.1039/C2GC35184F.
[20] G.-J. Kwon, D.-Y. Kim, S. Kimura and S. Kuga, Rapid-cooling, continuous-feed pyrolyzer for biomass processing: Preparation of levoglucosan from cellulose and starch; *Journal of Analytical and Applied Pyrolysis*, 80, (2007) 1-5, https://doi.org/10.1016/j.jaap.2006.12.012.
[21] E.B. Sanders, A.I. Goldsmith and J.I. Seeman, A model that distinguishes the pyrolysis of D-glucose, D-fructose, and sucrose from that of cellulose. Application to the understanding of cigarette smoke formation; *Journal of Analytical and Applied Pyrolysis*, 66, (2003) 29-50, https://doi.org/10.1016/S0165-2370(02)00104-3.
[22] V. Mamleev, S. Bourbigot, M. Le Bras and J. Yvon, The facts and hypotheses relating to the phenomenological model of cellulose pyrolysis: Interdependence of the steps; *Journal of Analytical and Applied Pyrolysis*, 84, (2009) 1-17, https://doi.org/10.1016/j.jaap.2008.10.014.
[23] Q. Lu, B. Hu, Z.-x. Zhang, Y.-t. Wu, M.-s. Cui, D.-j. Liu, C.-q. Dong and Y.-p. Yang, Mechanism of cellulose fast pyrolysis: The role of characteristic chain ends and dehydrated units; *Combustion and Flame*, 198, (2018) 267-277, https://doi.org/10.1016/j.combustflame.2018.09.025.
[24] J. Lédé, Cellulose pyrolysis kinetics: An historical review on the existence and role of intermediate active cellulose; *Journal of Analytical and Applied Pyrolysis*, 94, (2012) 17-32, https://doi.org/10.1016/j.jaap.2011.12.019.
[25] J. Lédé, F. Blanchard and O. Boutin, Radiant flash pyrolysis of cellulose pellets: products and mechanisms involved in transient and steady state conditions; *Fuel*, 81, (2002) 1269-1279, https://doi.org/10.1016/S0016-2361(02)00039-X.
[26] J.B. Paine III, Y.B. Pithawalla and J.D. Naworal, Carbohydrate pyrolysis mechanisms from isotopic labeling: Part 3. The Pyrolysis of d-glucose: Formation of C3 and C4 carbonyl compounds and a cyclopentenedione isomer by electrocyclic fragmentation mechanisms; *Journal of Analytical and Applied Pyrolysis*, 82, (2008) 42-69, https://doi.org/10.1016/j.jaap.2007.12.005.
[27] J.B. Paine III, Y.B. Pithawalla and J.D. Naworal, Carbohydrate pyrolysis mechanisms from isotopic labeling: Part 2. The pyrolysis of d-glucose: General disconnective analysis and the formation of C1 and C2 carbonyl compounds by electrocyclic fragmentation mechanisms; *Journal of Analytical and Applied Pyrolysis*, 82, (2008) 10-41, https://doi.org/10.1016/j.jaap.2008.01.002.
[28] J.B. Paine III, Y.B. Pithawalla and J.D. Naworal, Carbohydrate pyrolysis mechanisms from isotopic labeling: Part 4. The pyrolysis of d-glucose: The formation of furans; *Journal of Analytical and Applied Pyrolysis*, 83, (2008) 37-63, https://doi.org/10.1016/j.jaap.2008.05.008.
[29] G. Várhegyi, P. Szabó, W.S.-L. Mok and M.J. Antal, Kinetics of the thermal decomposition of cellulose in sealed vessels at elevated pressures. Effects of the presence of water on the reaction mechanism; *Journal of Analytical and Applied Pyrolysis*, 26, (1993) 159-174, https://doi.org/10.1016/0165-2370(93)80064-7.

[30] S.C. Moldoveanu and V. David, *Modern sample preparation for chromatography*, Elsevier, 2014, 311-318.

The role of water in pyrolysate composition and silylation efficiency during analytical reactive pyrolysis of glucans

Marco Mattonai*, Erika Ribechini

Department of Chemistry and Industrial Chemistry, University of Pisa, Via G. Moruzzi 13, 56124 Pisa, Italy

*corresponding author. Mail: m.mattonai@gmail.com

SUPPLEMENTARY MATERIAL

1. Pyrolysis apparatus

All pyrolysis experiments were performed using an EGA/Py-3030D micro-furnace pyrolyser equipped with a PY-1050 Micro Reaction Sampler (Frontier Laboratories Ltd., Japan). A scheme of the apparatus with a close-up of the Micro Reaction Sampler is provided in Figure S1. The pyrolysis furnace consists of a deactivated steel tube with an internal diameter of 4 mm. The pyrolysis furnace temperature was 400 °C in all experiments, while the temperature of the interface with the GC/MS system was 280 °C. These temperatures were measured using the internal measuring system of the instrument (1 °C error).

Before each experiment, 80 μg of sample are weighted in a glass vial approximately 40 mm in length and with an internal diameter of approximately 1.5 mm, and 3 μL of derivatising agent (hexamethyldisilazane) are added. The vial is then put under a gentle stream of nitrogen to remove oxygen, and then it is flame-sealed and placed at the top of the pyrolysis furnace using a steel sample holder, as shown in Figure 2Sc. The sample holder is equipped with a crushing steel rod connected to a rotating knob at the top of the micro reaction sampler. At the start of the analysis, the sample holder is lowered in the pyrolysis furnace. The sample heating rate for a Frontier Laboratories pyrolyser has been estimated in previous publications to be approximately 180 °C/s [1]. The use of a micro reaction sampler allows pyrolysis temperatures up to 400 °C to be employed.

Higher temperatures can lead to excessive pressure inside the glass vial, with the risk of premature shattering. With the specified sample amounts, and assuming an average volume of 50 µL of the glass vial, the pressure in the glass vial during pyrolysis can be estimated to be approximately 2 MPa.

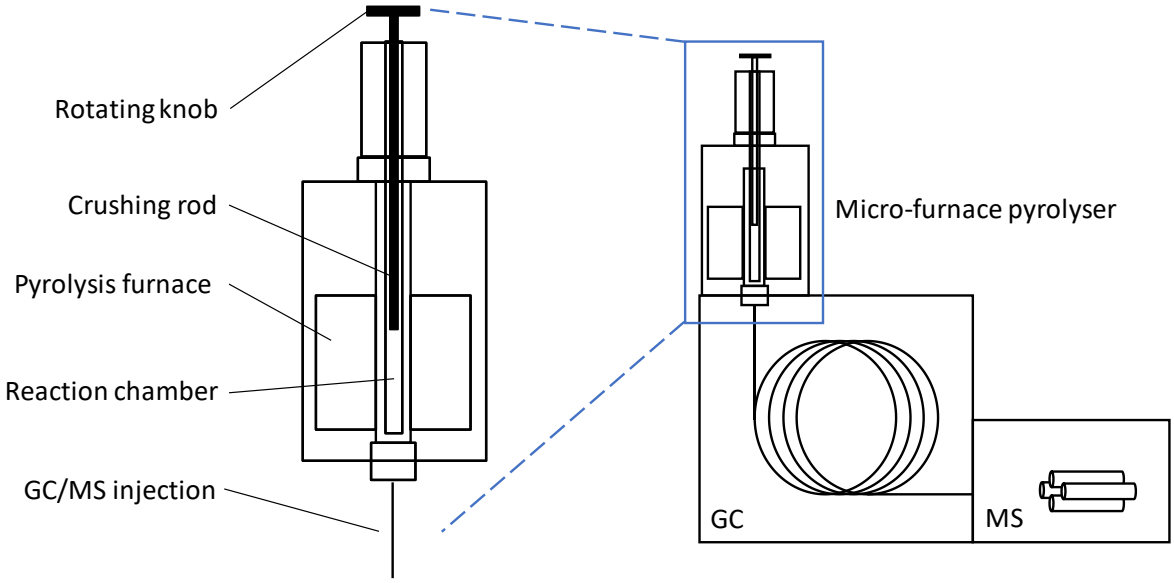

Figure S1: Scheme of the Py-GC/MS apparatus and close-up of the microfurnace pyrolyser with micro reaction sampler.

The pyrolysis of the sample is carried out for the desired amount of time, after which the knob is manually rotated to lower the crushing rod. The rod crushes the glass vial, freeing the pyrolysis products who are carried to the GC/MS system. The sample holder presents holes at its bottom, to allow for an efficient transfer of the pyrolysis products. The residence time of the pyrolysis vapours inside the furnace in a Frontier Laboratories pyrolyser was estimated in previous publications to be approximately 10 s [2].

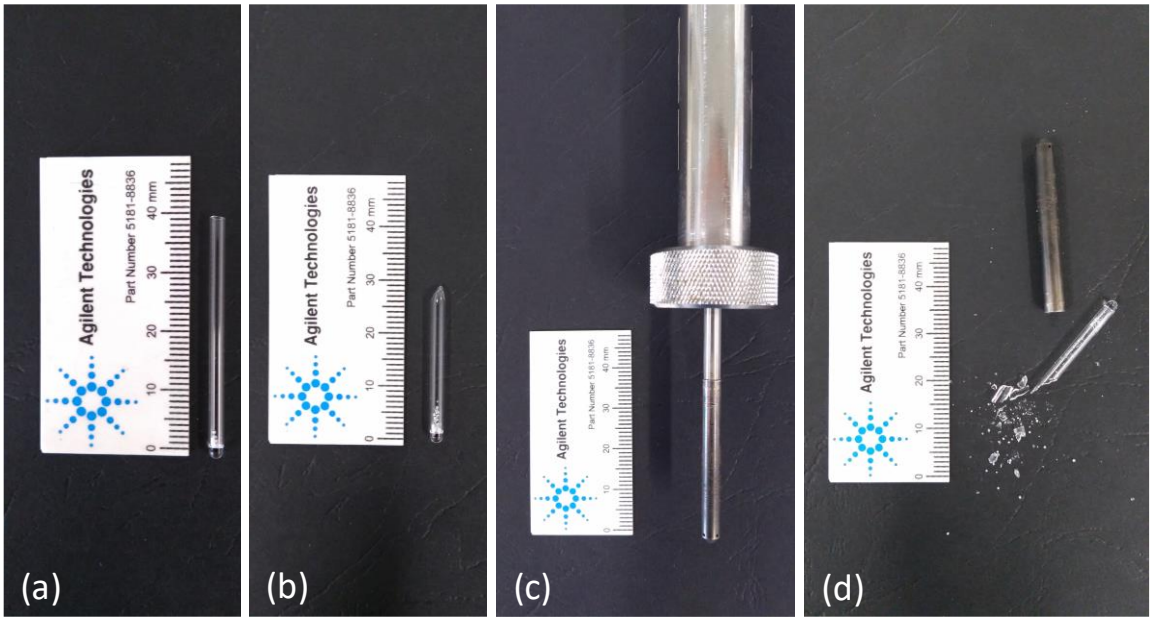

Figure S2: (a) glass capsule with sample before flame-sealing; (b) glass capsule after flame-sealing; (c) sample holder used for reactive pyrolysis; (d) shattered glass capsule after the analysis.

2. Identified Compounds

A list of all the identified compounds is presented in Table S1. Identification of each compound was based on its mass spectrum, using two reference mass spectra libraries (NIST/EPA/NIH 2002 and Wiley 275) and three previous literature publications [3-5] as comparison. All identified compounds were grouped into six categories based on their structure: small molecules (Smo), cyclopentenones (Cyp), furans (Fur), pyrans (Pyr), hydroxybenzenes (Hyb) and anhydrosugars (Ahs). Compounds that did not belong in any of these categories were labelled as "other compounds" (Oth).

Table S1: List of all identified compounds in the pyrograms of cellobiose and cellohexose at all pyrolysis times. Compounds are listed according to their relative retention order. For each compound, the number of trimethylsilyl groups (TMS), the compound category (Cat) and the main *m/z* signals in the mass spectrum are displayed. Smo = small molecules, Cyp = cyclopentenones, Fur = furans, Pyr = pyrans, Hyb = hydroxybenzenes, Ahs = anhydrosugars, Oth = other compounds.

#	Compound	Cat	*m/z*
1	2-hydroxymethylfuran (TMS)	Fur	75, 81, 111, 125, 142, 155, 170
2	hydroxyacetaldehyde, enolic form I (2TMS)	Smo	73, 147, 189, 204
3	hydroxyacetone, enolic form I (2TMS)	Smo	73, 100, 147, 188, 203
4	phenol (TMS)	Hyb	73, 151, 166
5	2-hydroxypropanoic acid (2TMS)	Smo	73, 117, 133, 147, 190, 219
6	hydroxyacetic acid (2TMS)	Smo	73, 133, 147, 161, 177, 205, 220

7	pyruvic acid, enolic form (2TMS)	Smo	73, 100, 114, 128, 147, 217
8	hydroxyacetone, enolic form II (2TMS)	Smo	73, 100, 116, 147, 188, 203
9	3-oxopropanoic acid, enolic form I (2TMS)	Smo	73, 114, 129, 147, 191, 217
10	hydroxyacetaldehyde, enolic form II (2TMS)	Smo	73, 147, 189, 204
11	2-furancarboxylic acid (TMS)	Fur	73, 95, 125, 169, 184
12	1,2-cyclopentadione, enolic form (TMS)	Cyp	73, 75, 81, 111, 155
13	3-hydroxypropanoic acid (2TMS)	Smo	73, 147, 177, 219
14	3-hydroxycyclopenta-1,2-dione (TMS)	Cyp	73, 115, 129, 143, 171, 186
15	2-hydroxycyclopenta-1,3-dione (TMS)	Cyp	73, 75, 101, 143, 171
16	3-hydroxy-4H-pyran-4-one (TMS)	Pyr	75, 95, 147, 169, 184
17	5-hydroxy-2H-pyran-4(*3H*)-one (TMS)	Pyr	73, 75, 101, 129, 143, 171, 186
18	2-hydroxymethyl-3-methyl-cyclopentenone (TMS)	Cyp	73, 193, 198
19	6-hydroxy-2-methyl-*4H*-pyran-4-one (TMS)	Pyr	73, 117, 147, 183, 198
20	2-methylcyclopenta-1,3-dione, enolic form (TMS)	Cyp	75, 117, 139, 169, 184
21	3-methylcyclopenta-1,2-dione, enolic form (TMS)	Cyp	73, 97, 169, 184
22	1,3-dihydroxyacetone (2TMS)	Smo	73, 103, 129, 147, 189, 219
23	3-hydroxy-6-methyl-*2H*-pyran-2-one (TMS)	Pyr	75, 168, 183, 198
24	glycerol (3TMS)	Smo	73, 103, 117, 133, 147, 205, 218
25	2-methyl-3-hydroxymethyl-2-cyclopentenone (TMS)	Cyp	55, 69, 83, 97, 153, 183, 198
26	2,3-dihydrofuran-2,3-diol (2TMS)	Fur	73, 147, 157, 231, 246
27	5-hydroxymethyl-2-furaldehyde (TMS)	Fur	73, 109, 139, 169, 183, 198
28	1,2-dihydroxybenzene (2TMS)	Hyb	73, 151, 239, 254
29	3-hydroxycyclopenta-1,2-dione, enolic form (2TMS)	Cyp	73, 133, 147, 169, 230, 243, 258
30	2,3-dihydroxypropanoic acid (3TMS)	Smo	73, 103, 117, 133, 147, 189, 205, 292, 307
31	3-hydroxy-2-hydroxymethyl tetrahydropyran (2TMS)	Pyr	73, 103, 129, 147, 173, 191, 204, 217, 231, 276
32	1,4:3,6-dianhydroD-glucopyranose (TMS)	Ahs	59, 69, 73, 81, 85, 103, 117, 129, 145, 155, 170
33	2-hydroxycyclopenta-1,3-dione, enolic form (2TMS)	Cyp	73, 243
34	1,4-dihydroxybenzene (2TMS)	Hyb	73, 239, 254
35	5-formyltetrahydrofuran-2-carboxylic acid (TMS)	Fur	73, 75, 129, 143, 173
36	n-hydroxy-n'-hydroxymethyl-*2H*-pyran-4(*3H*)-one (2TMS)	Pyr	73, 129, 147, 155, 183, 273, 288
37	arabinofuranose (4TMS)	Oth	73, 103, 129, 143, 147, 217, 230
38	2-(1,2-dihydroxyethyl)furan (2TMS)	Fur	73, 147, 169, 183, 257, 272
39	3-hydroxy-2-(hydroxymethyl)cyclopent-2-enone (2TMS)	Cyp	73, 257, 272
40	2-hydroxycyclopenta-1,3-dione, enolic form (2TMS)	Cyp	73, 133, 147, 228, 243, 258
41	3,5-dihydroxy-2-methyldihydro-*4H*-pyran-4-one (2TMS)	Pyr	73, 101, 147, 155, 183, 273, 288
42	3-hydroxycyclopenta-1,2-dione, enolic form (2TMS)	Cyp	73, 147, 230, 243, 258
43	3-hydroxy-2-(hydroxymethyl)cyclopenta-2,4-dienone (2TMS)	Cyp	73, 147, 255, 270
44	1,2,5-trihydroxypentane (3TMS)	Oth	73, 85, 133, 143, 147, 233
45	3,5-dihydroxy-2-methyl-*4H*-pyran-4-one (2TMS)	Pyr	73, 128, 199, 271, 286
46	1,6-anhydro-β-glucopyranose (TMS C4)	Ahs	73, 103, 117, 129, 145, 155, 171
47	1,6-anhydro-β-glucopyranose (TMS C2)	Ahs	73, 101, 116, 129, 132, 145, 155, 171
48	2-deoxyribono-1,4-lactone (2TMS)	Oth	73, 97, 103, 147, 189, 219, 261
49	2-methyl-3-hydroxycyclopentanone, enolic form (2TMS)	Cyp	73, 103, 147, 169, 185, 243, 258
50	1,2,3-trihydroxybenzene (3TMS)	Hyb	73, 239, 342
51	1,4-anhydro-D-galactopyranose (2TMS)	Ahs	73, 101, 116, 129, 145, 155, 189, 204, 217
52	1,6-anhydro-D-galactopyranose (2TMS)	Ahs	73, 101, 116, 129, 145, 161, 189, 204, 217

53	2-hydroxymethyl-5-hydroxy-2,3-dihydro-4H-pyran-4-one (2TMS)	Pyr	73, 129, 155, 183, 273, 288
54	1,4-anhydro-D-glucopyranose (2TMS)	Ahs	73, 129, 147, 157, 191, 217
55	1,2,4-trihydroxybenzene (3TMS)	Hyb	73, 239, 342
56	1,6-anhydro-β-D-glucopyranose (2TMS)	Ahs	73, 101, 116, 129, 155, 191, 204, 217, 230
57	xylonic acid γ-lactone (3 TMS)	Oth	73, 103, 117, 147, 189, 204, 217, 231, 246, 259, 349, 364
58	4,5-dihydroxy-2-hydroxymethyl-*2H*-pyrane (3TMS)	Pyr	73, 103, 133, 147, 257, 330, 345, 360
59	2,3-dihydroxy-6-methyl-*4H*-pyran-4-one (2TMS)	Pyr	73, 147, 169, 271, 286
60	2,3,5-trihydroxy-*4H*-pyran-4-one (3TMS)	Pyr	73, 103, 133, 147, 255, 330, 345, 360
61	1,6-anhydro-β-D-glucopyranose (3TMS)	Ahs	73, 103, 129, 147, 191, 204, 217, 243, 333
62	1,4-anhydro-D-glucopyranose (3TMS)	Ahs	73, 103, 117, 129, 147, 157, 191, 204, 217, 243, 332
63	1,6-anhydro-β-D-glucofuranose (3TMS)	Ahs	73, 101, 116, 129, 147, 157, 191, 217, 243, 319
64	ribonic acid γ-lactone (3TMS)	Oth	73, 103, 117, 129, 147, 205, 246, 273, 292, 363, 378
65	arabinonic acid γ-lactone (3TMS)	Oth	73, 103, 117, 129, 147, 205, 246, 273, 292
66	L-altrose (5TMS)	Oth	73, 147, 191, 205, 217, 319
67	3,4,5-trihydroxy-6-(hydroxymethyl)-tetrahydro-2H-pyran-2-one (4TMS)	Pyr	73, 103, 129, 147, 204, 220, 229, 319
68	gluconic acid δ-lactone (4TMS)	Oth	73, 103, 129, 147, 189, 204, 217, 230, 244, 305, 333, 361
69	unknown glucopyranose (5TMS)	Oth	73, 103, 117, 129, 147, 191, 204, 217, 231, 246, 273, 363

Twelve representative mass spectra of identified compounds are presented in Figure S3.

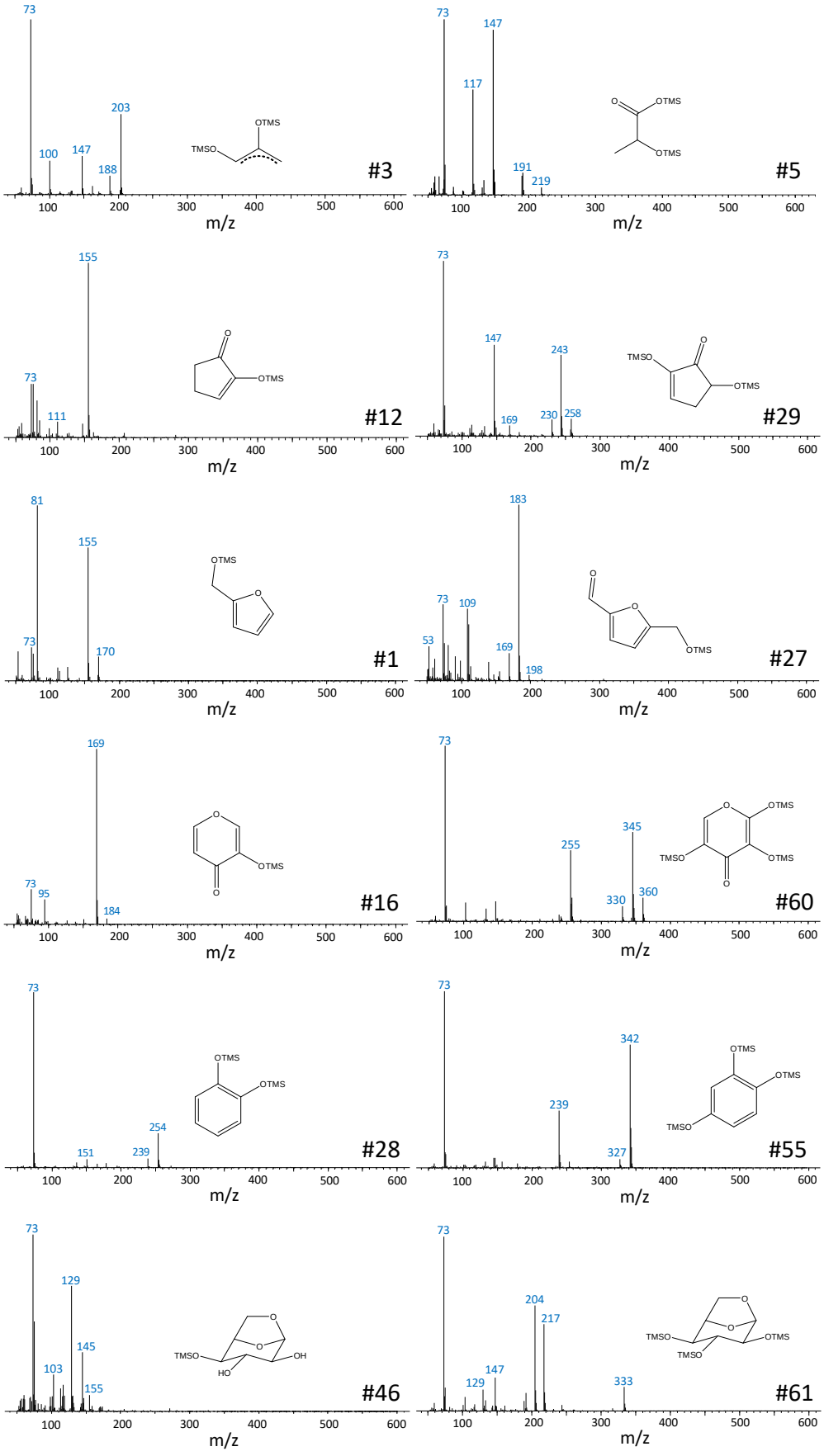

432

Figure S3: Representative mass spectra of twelve identified pyrolysis products. The structure and compound number according to Table S1 are displayed for each compound. Each row corresponds to one of the six main compound categories: from top to bottom - small molecules, cyclopentenones, furans, pyrans, hydroxybenzenes, anhydrosugars.

Two pyrograms for both cellobiose and cellohexose are displayed in Figure S3 and Figure S4, respectively. The pyrograms obtained after 0.5 and 30 min of pyrolysis were chosen as representatives of a short and a long pyrolysis time.

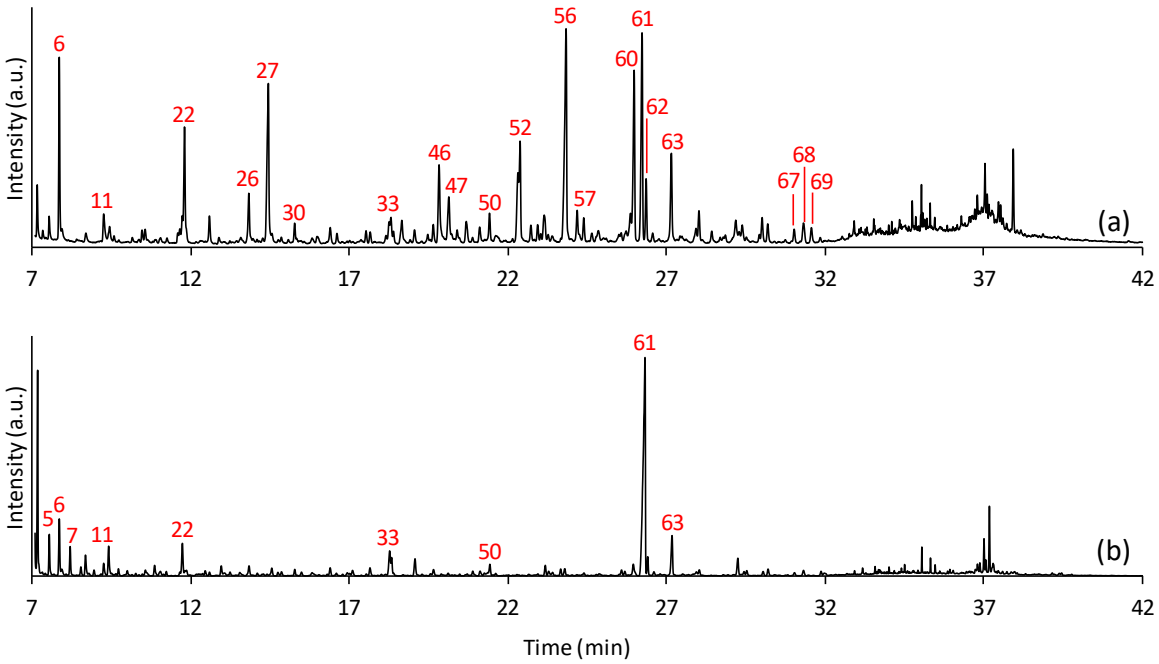

Figure S3: Pyrograms obtained for cellobiose after 0.5 min (a) and 30 min (b) of pyrolysis. The main peaks of identified compounds are labelled according to Table S1.

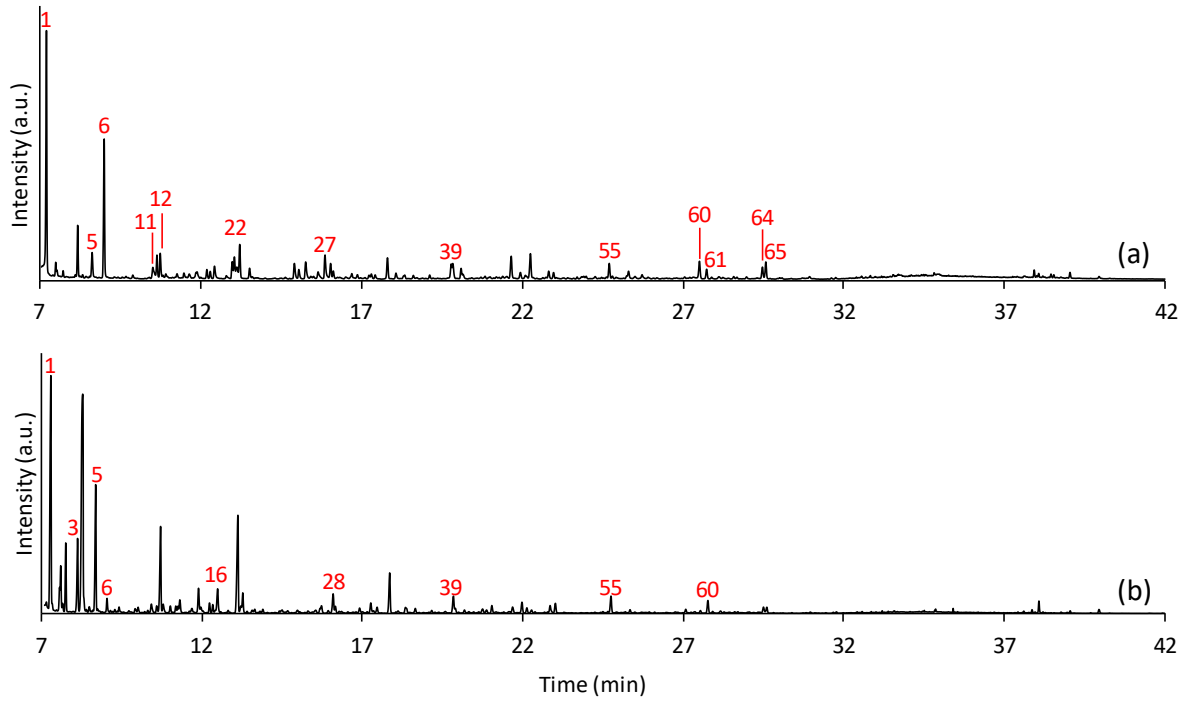

Figure S4: Pyrograms obtained for cellohexose after 0.5 min (a) and 30 min (b) of pyrolysis. The main peaks of identified compounds are labelled according to Table S1.

3. Semi-quantitative analysis

Semi-quantitative analyses were carried out using the integrated areas of all identified peaks. The areas were converted into percentages dividing by the total area of each pyrogram. All percentage areas for cellobiose and cellohexose are presented in Tables S2 and S3, respectively. The relative standard deviation on these values was evaluated by performing replicates at the same pyrolysis time, and was found to be lower than 10%. The total percentage area for each compound category is obtained by adding together all percentage areas of its members.

Table S2: Percentage areas of all identified compounds in the pyrograms of cellobiose at all pyrolysis times.

		Pyrolysis time (min)								
Compound	**Cat**	**0.2**	**0.5**	**1**	**2**	**5**	**10**	**20**	**30**	**60**
phenol	Hyb	0.4	0.2	0.4	0.2	0.1	0	0	0	0
hydroxyacetic acid (2TMS)	Smo	8.3	6.8	8	7.1	7.8	6.4	6.6	6.7	5.6
pyruvic acid, enolic form (2TMS)	Smo	0	0	0	0.2	0.8	1.7	2.5	3.6	4.8
hydroxyacetone, enolic form II (2TMS)	Smo	0	0	0	0	0.4	0.9	0	1	1.4
3-oxopropanoic acid, enolic form (2TMS)	Smo	0	0.3	0.3	0.9	1.1	1.7	2	2.7	2.9

hydroxyacetaldehyde, enolic form II (2TMS)	Smo	1.8	1.2	0.6	0.6	0	0	0	0	0
2-furancarboxylic acid (TMS)	Fur	0.7	0.6	0.8	0.7	0.9	0.8	0.9	1	0.8
1,2-cyclopentadione, enolic form (TMS)	Cyp	1	0	0	0	0	0	0	0	0
3-hydroxypropanoic acid (2TMS)	Smo	0.2	0.2	0.2	0.2	0.2	0.2	0.1	0	0
3-hydroxycyclopenta-1,2-dione (TMS)	Cyp	0.9	0.4	0.4	0.3	0	0	0	0	0
3-hydroxy-*4H*-pyran-4-one (TMS)	Pyr	0.2	0.1	0.2	0.1	0.3	0.2	0.3	0.5	0.6
5-hydroxy-*2H*-pyran-4(*3H*)-one (TMS)	Pyr	0	0	0.1	0	0	0	0	0	0
2-hydroxymethyl-3-methyl-cyclopentenone (TMS)	Cyp	0.7	0.2	0.1	0	0	0	0	0	0
2-methylcyclopentan-1,3-dione, enolic form (TMS)	Cyp	0.4	0	0	0	0	0	0	0	0
3-methylcyclopenta-1,2-dione, enolic form (TMS)	Cyp	0.3	0.1	0.2	0.1	0.1	0.1	0.1	0.2	0
1,3-dihydroxyacetone (2TMS)	Smo	7.5	5.5	5.6	5.1	0	0	0	0	0
glycerol (3TMS)	Smo	0	0.1	0.1	0.1	0.2	0.3	0.3	0.4	0.5
2-methyl-3-hydroxymethyl-2-cyclopentenone (TMS)	Cyp	0.2	0.3	0.2	0.2	0.2	0	0	0	0
2,3-dihydrofuran-2,3-diol (2TMS)	Fur	1.8	3.8	2.7	3.8	3.6	2.7	1.9	1.3	0.9
5-hydroxymethyl-2-furaldehyde (TMS)	Fur	11.1	9.5	10.2	7.7	5.9	2.4	0.6	0	0
1,2-dihydroxybenzene (2TMS)	Hyb	0	0.2	0.3	0.4	0	0	0	0	1.2
3-hydroxycyclopenta-1,2-dione, enolic form (2TMS)	Cyp	0.1	0.1	0.1	0.2	0.1	0.1	0	0	0
2,3-dihydroxypropanoic acid (3TMS)	Smo	0.8	0.9	0.9	0.9	1	1	1.1	0.9	0.6
1:4,3:6-anhydro-α-D-glucopyranose (TMS)	Ahs	0	0	0.1	0	0	0	0.1	0	0
2-hydroxycyclopenta-1,3-dione, enolic form (2TMS)	Cyp	0	0	0	0.3	0	0	0	0	0
1,4-dihydroxybenzene (2TMS)	Hyb	0.1	0	0.1	0	0.1	0.1	0.1	0.2	0.3
2-(1,2-dihydroxyethyl)-furan (2TMS)	Fur	0.4	0	0.3	0	0	0	0	0	0
3-hydroxy-2-hydroxymethyl-2-cyclopentenone (2TMS)	Cyp	0.6	0.8	0.6	0.6	1.1	1.8	3.2	4.7	6.3
2-hydroxycyclopenta-1,3-dione, enolic form (2TMS)	Cyp	0.5	0.7	0.7	1.1	1.6	1.6	1.3	1.9	2.2
3,5-dihydroxy-2-methyldihydro-*4H*-pyran-4-one (2TMS)	Pyr	0.2	0.4	1.1	0.7	0.7	0.4	0.2	3.2	1.9
3-hydroxy-2-hydroxymethylcyclopenta-2,4-dienone (2TMS)	Cyp	0.5	0.7	0.8	1.2	2	2.7	3.1	0	0.7
1,2,5-trihydroxypentane (3TMS)	Oth	0	0	0	0	0	0	0	0.1	0
3,5-dihydroxy-2-methyl-*4H*-pyran-4-one (2TMS)	Pyr	0.8	0.8	0.8	0.6	1	1	1.2	0.9	0
1,6-anhydro-β-D-glucopyranose (TMS C4)	Ahs	3.3	1.6	0	0	0	0	0	0	0
1,6-anhydro-β-D-glucopyranose (TMS C2)	Ahs	3.6	2.1	2.3	1	0	0	0	0	0
2-deoxy-D-ribono-1,4-lactone (2TMS)	Oth	0.7	0.3	0.3	0.4	0	0	0	0	0
2-methyl-3-hydroxycyclopentanone, enolic form (2TMS)	Cyp	0.8	0.8	0.5	0.7	0	0	0	0	0
1,2,3-trihydroxybenzene (3TMS)	Hyb	0.6	1.1	1.3	1.3	1.5	1.5	1.5	1.7	2.3
1,4-anhydro-D-galactopyranose (2TMS)	Ahs	4.4	3.2	3.4	2	1.2	0	0	0	0
1,6-anhydro-D-galactopyranose (2TMS)	Ahs	4.3	4	5.4	2.9	1.4	0.3	1.5	0	0
2-hydroxymethyl-5-hydroxy-2,3-dihydro-*4H*-pyran-4-one (2TMS)	Pyr	1.5	0.7	0.5	0.4	0.2	0	0	0	0
1,4-anhydro-β-D-glucopyranose (2TMS)	Ahs	0.8	0.4	1.8	0.5	0	0	0	0	0
1,2,4-trihydroxybenzene (3TMS)	Hyb	1	0.7	0.5	0.8	1	1.1	0	1.7	2.4
1,6-anhydro-β-D-glucopyranose (2TMS)	Ahs	12.2	16.2	13.4	12.6	11.9	6.4	0	0	0
4,5-dihydroxy-2-hydroxymethyl-(*2H*)-pyrane (3TMS)	Pyr	0.8	1.3	1.1	1.7	1.2	1.1	0.6	0.2	0

2,3-dihydroxy-6-methyl-*4H*-pyran-4-one (2TMS)	Pyr	0.2	0.1	0	0.5	0.2	0.4	0	0	0
2,3,5-trihydroxy-*4H*-pyran-4-one (3TMS)	Pyr	12.9	11.4	8.5	11.2	8.3	6.3	4	1.7	0.2
1,6-anhydro-β-D-glucopyranose (3TMS)	Ahs	3.3	10.6	13.6	17.3	31.2	40.2	53.2	53.5	53.6
1,4-anhydro-β-D-glucopyranose (3TMS)	Ahs	3.5	2.5	2.4	2.3	2	2.2	2.4	2.4	2.5
1,6-anhydro-β-D-glucofuranose (3TMS)	Ahs	2.4	4.2	4.6	4.6	7.1	6.5	7.9	7.1	6.5
riboic acid γ-lactone	Oth	1.5	1.3	0.4	0.4	0.5	1.1	0.4	0.2	0.3
arabinoic acid γ-lactone	Oth	0	0	1.2	0	0	2.1	0	0	0
L-altrose (5TMS)	Oth	0.3	1.1	1	2	1.6	1.7	1.1	1	0.5
3,4,5-trihydroxy-6-(hydroxymethyl)-tetrahydro-*2H*-pyran-2-one (4TMS)	Pyr	0.1	0	0.8	1.8	1.2	1.3	0.7	0.4	0.3
gluconic acid δ-lactone	Oth	0.9	1.2	0.9	1.7	0.1	1.3	1	0.9	0.6
unknown glucopyranose	Oth	1.3	0.9	0.4	0.5	0.5	0.4	0	0	0

Table S3: Percentage areas of all identified compounds in the pyrograms of cellohexose at all pyrolysis times.

		Pyrolysis time (min)								
Compound	**Cat**	**0.2**	**0.5**	**1**	**2**	**5**	**10**	**20**	**30**	**60**
2-hydroxymethylfuran (TMS)	Fur	40.5	37.1	37.5	39.3	46.1	44.3	47.6	49.1	51.7
hydroxyacetaldehyde, enolic form (2TMS)	Smo	0.1	0.6	1.3	1.5	2.1	3.4	5.1	5	3.8
hydroxyacetone, enolic form I (2TMS)	Smo	0	0	0.2	1.3	1.6	4	8.3	8.4	9.4
2-hydroxypropanoic acid, enolic form (2TMS)	Smo	0	0	0.1	0.5	1	0	0	7.4	6.2
hydroxyacetic acid (2TMS)	Smo	18.6	23	14.1	15.1	10.5	6.5	3.2	0.2	0
pyruvic acid, enolic form (2TMS)	Smo	0	0	0	0	0	0.2	0.5	0.7	0.8
hydroxyacetone, enolic form II (2TMS)	Smo	0	0	0	0.2	0.1	0.2	0.4	0.1	0.9
2-furancarboxylic acid (TMS)	Fur	1.4	1.7	1	1.2	0.7	0.4	0.2	0	0
1,2-cyclopentadione, enolic form (TMS)	Cyp	3.8	4.4	4.8	4.8	4.2	3.6	2.8	0	0
3-hydroxypropanoic acid (2 TMS)	Smo	0.3	0.3	0.1	0.2	0.1	0.1	0	0	0
3-hydroxycyclopenta-1,2-dione (TMS)	Cyp	0.2	0.1	0.1	0	0	0	0	0	0
3-hydroxy-*4H*-pyran-4-one (TMS)	Pyr	0.8	2.4	2.4	2.7	3.3	4.3	5.3	5.2	3.1
2-hydroxymethyl-3-methyl-cyclopentenone (TMS)	Cyp	0.2	0	0	0	0	0	0	0	0
3-methylcyclopenta-1,2-dione, enolic form (TMS)	Cyp	0.7	0.2	0	0.1	0	0	0	0	0
1,3-dihydroxyacetone (2TMS)	Smo	2.1	0.4	0.5	0.3	0	0.5	0	0	0
3-hydroxy-6-methyl-*2H*-pyran-2-one (TMS)	Pyr	0.2	0.3	0.1	0.2	0.1	0.5	0.6	0.5	0.3
glycerol (3 TMS)	Smo	0	0	0	0	0	0	0.4	0.3	0.3
2-methyl-3-hydroxymethyl-2-cyclopentenone (TMS)	Cyp	1.4	1.9	1.2	0.9	0.8	1	0.2	0	0
2,3-dihydrofuran-2,3-diol (2 TMS)	Fur	1.8	0	2.5	1.4	0	0.6	0	0	0
5-hydroxymethyl-2-furaldehyde (TMS)	Fur	3.6	4.8	3.3	2.5	2	4.2	0	0	0
1,2-dihydroxybenzene (2 TMS)	Hyb	1.8	2.7	3.2	4	4.1	0	4.6	5.6	6.4
3-hydroxycyclopenta-1,2-dione, enolic form (2TMS)	Cyp	0	0	0.2	0.2	0.1	0.3	0	0	0
2,3-dihydroxypropanoic acid (3TMS)	Smo	1.2	0.8	0.9	0.8	0.8	0	0.1	0	0
1:4,3:6-anhydro-α-D-glucopyranose (TMS)	Oth	0.2	0	0	0	0	0.9	0	0	0
1,4-dihydroxybenzene (2TMS)	Hyb	0.4	0.6	0.5	0.5	0.5	0.6	1	1.4	1.3
2-(1,2-dihydroxyethyl)furan (2TMS)	Fur	0.7	0.6	0.6	0.4	0.5	6.6	0.6	0.7	0.6

3-hydroxy-2-hydroxymethyl-2-cyclopentenone (2TMS)	Cyp	1.8	2.4	3.6	3.1	3.3	0.6	4.7	2	1
2-hydroxycyclopenta-1,3-dione, enolic form (2TMS)	Cyp	0.4	0.4	0.7	0	2	0	0.4	0	0
3,5-dihydroxy-2-methyldihydro-*4H*-pyran-4-one (2TMS)	Pyr	0.1	0	0.2	0	0.1	0	0	0	0
3-hydroxycyclopenta-1,2-dione, enolic form (2TMS)	Cyp	0	0	0.1	0	0	0	0	0	0
3-hydroxy-2-hydroxymethylcyclopenta-2,4-dienone (2TMS)	Cyp	0.2	0.1	0.1	0.2	0.2	0.1	0.1	0	0
1,2,5-trihydroxypentane (3TMS)	Oth	0.7	0.6	1.3	1.4	1.1	1.1	0.9	0.4	0.3
3,5-dihydroxy-2-methyl-*4H*-pyran-4-one (2TMS)	Pyr	0.3	0.2	0.2	0.2	0.2	0.1	0.1	0	0
1,2,3-trihydroxybenzene (3TMS)	Hyb	1.1	1.1	1.9	1.7	2	2.1	2.4	2.9	2.6
1,4-anhydro-D-galactopyranose (2TMS)	Ahs	0.3	0.2	0.1	0	0	0	0	0	0
1,6-anhydro-D-galactopyranose (2TMS)	Ahs	0.3	0.4	0.2	0.1	0.1	0	0	0	0
2-hydroxymethyl-5-hydroxy-2,3-dihydro-*4H*-pyran-4-one (2TMS)	Pyr	0.5	0.1	0.1	0.1	0.1	0	0	0	0
1,2,4-trihydroxybenzene (3TMS)	Hyb	3.4	2.8	3.6	3.4	3.1	3.5	4	4.5	4.4
1,6-anhydro-β-D-glucopyranose (2TMS)	Ahs	1	1.7	1.4	1	0.6	0.4	0.4	0.4	0.4
4,5-dihydroxy-2-hydroxymethyl-*2H*-pyrane (3TMS)	Pyr	0	0	0.1	0	0	0	0	0	0
2,3,5-trihydroxy-*4H*-pyran-4-one (3TMS)	Pyr	7.3	3.6	5.9	5.4	3.2	2.1	0.9	0	0
1,6-anhydro-β-D-glucopyranose (3TMS)	Ahs	0.4	1.7	2.3	2.2	2.9	3.2	2.9	3.4	5.3
1,4-anhydro-β-D-glucopyranose (3TMS)	Ahs	0.2	0.1	0.3	0.2	0.1	0.1	0.2	0.2	0.2
1,6-anhydro-β-D-glucofuranose (3TMS)	Ahs	0.1	0.2	0.3	0.2	0.2	0.2	0.2	0.2	0.3
riboic acid γ-lactone	Oth	1.6	2.2	2.5	2	2	1.8	1.5	1.1	0.6
arabinoic acid γ-lactone	Oth	0	0	0	0	0	2.1	0	0	0
L-altrose (5TMS)	Oth	0	0.2	0.4	0.4	0.2	0.2	0.2	0.1	0
3,4,5-trihydroxy-6-(hydroxymethyl)tetrahydro-*2H*-pyran-2-one (4TMS)	Pyr	0	0.2	0.1	0.1	0.2	0.1	0	0.1	0
gluconic acid δ-lactone	Oth	0	0	0.1	0.2	0	0.1	0.1	0	0
unknown glucopyranose	Oth	0.2	0	0.1	0.1	0	0	0.1	0	0

REFERENCES

[1] S. Maduskar, G.G. Facas, C. Papageorgiou, C.L. Williams and P.J. Dauenhauer, Five rules for measuring biomass pyrolysis rates: pulse-heated analysis of solid reaction kinetics of lignocellulosic biomass; *ACS Sustainable Chemistry & Engineering*, 6, (2017) 1387-1399, https://doi.org/10.1021/acssuschemeng.7b03785.

[2] J. Proano-Aviles, J.K. Lindstrom, P.A. Johnston and R.C. Brown, Heat and Mass Transfer Effects in a Furnace-Based Micropyrolyzer; *Energy Technology*, 5, (2017) 189-195, https://doi.org/10.1002/ente.201600279.

[3] D. Fabbri and G. Chiavari, Analytical pyrolysis of carbohydrates in the presence of hexamethyldisilazane; *Analytica Chimica Acta*, 449, (2001) 271-280, https://doi.org/10.1016/S0003-2670(01)01359-9.

[4] D. Tamburini, J.J. Łucejko, M. Zborowska, F. Modugno, W. Prądzyński and M.P. Colombini, Archaeological wood degradation at the site of Biskupin (Poland): wet chemical analysis and evaluation of specific Py-GC/MS profiles; *Journal of Analytical and Applied Pyrolysis*, 115, (2015) 7-15, https://doi.org/10.1016/j.jaap.2015.06.005.

[5] M. Mattonai, D. Tamburini, M.P. Colombini and E. Ribechini, Timing in Analytical Pyrolysis: Py(HMDS)-GC/MS of Glucose and Cellulose Using Online Micro Reaction Sampler; *Analytical Chemistry*, 88, (2016) 9318-9325, https://doi.org/10.1021/acs.analchem.6b02910.